

Rapid and Robust Detection Methods for Poison and Microbial Contamination

Melanie M. Hoehl,^{*,†,‡} Peter J. Lu,[#] Peter A. Sims,[§] and Alexander H. Slocum[†]

[†]Department of Mechanical Engineering, Massachusetts Institute of Technology, Cambridge, Massachusetts 02139, United States

[‡]Harvard–MIT Division of Health Sciences and Technology, Cambridge, Massachusetts 02139, United States

[#]Department of Physics and SEAS, Harvard University, Cambridge, Massachusetts 02138, United States

[§]Columbia Initiative in Systems Biology, Department of Biochemistry and Molecular Biophysics, Columbia University Medical Center, New York, New York 10032, United States

S Supporting Information

ABSTRACT: Real-time on-site monitoring of analytes is currently in high demand for food contamination, water, medicines, and ingestible household products that were never tested appropriately. Here we introduce chemical methods for the rapid quantification of a wide range of chemical and microbial contaminations using a simple instrument. Within the testing procedure, we used a multichannel, multisample, UV–vis spectrophotometer/fluorometer that employs two frequencies of light simultaneously to interrogate the sample. We present new enzyme- and dye-based methods to detect (di)ethylene glycol in consumables above 0.1 wt % without interference and alcohols above 1 ppb. Using DNA intercalating dyes, we can detect a range of pathogens (*E. coli*, *Salmonella*, *V. Cholera*, and a model for Malaria) in water, foods, and blood without background signal. We achieved universal scaling independent of pathogen size above 10⁴ CFU/mL by taking advantage of the simultaneous measurement at multiple wavelengths. We can detect contaminants directly, without separation, purification, concentration, or incubation. Our chemistry is stable to ±1% for >3 weeks without refrigeration, and measurements require <5 min.

KEYWORDS: UV absorption, fluorescence, detection, ethylene glycol, diethylene glycol, malaria, food pathogens, *Salmonella*, *E. coli*, *V. cholera*

INTRODUCTION

Contamination of food, water, medicine, and ingestible household consumer products is a public health hazard that episodically causes thousands of deaths and each year sickens millions worldwide.^{1,2} For example, lower cost ethylene glycol (EG) and diethylene glycol (DEG) have been substituted for the nontoxic glycerol, propylene glycol, and polyethylene glycol often used in medicines, household products, and foods.^{3,4} Ingestion of even a small amount of EG or DEG can result in central nervous system depression, cardiopulmonary compromise, and kidney failure.^{5–8} A longstanding problem that led to the 1938 Food, Drug and Cosmetic Act established the modern drug-approval process within the U.S. Food and Drug Administration (FDA).⁹ DEG contamination remains a serious hazard today.³ In the past 15 years, episodes of DEG poisoning have killed hundreds, particularly in developing countries.^{5,8–21} In addition to chemical poisoning, contamination of food and water by microbes such as *Escherichia coli* and *Salmonella* in food^{2,22–25} or *Vibrio cholera* in water^{26,27} sickens millions (see the Supporting Information for recent contamination data).

Existing laboratory methods to detect many common relevant chemicals and pathogens (such as GC, MS, optical spectroscopy, or electrochemistry^{5,31,33–36}) require specialized scientific equipment, a stable laboratory environment, a continuous refrigeration chain for reagents or antibodies, and/or specially trained staff,^{28–33} all of which are expensive and generally preclude their use at the location of an outbreak or natural disaster.³⁴ Any detector for field use should rely on a

simpler, more mechanically robust technology. There has thus been an effort to develop field-deployable diagnostic technologies (e.g., microfluidic, nanotechnology, or surface plasmon resonance methods) that can be used outside a stable laboratory environment. For the past 7 years, this has led to numerous publications about early-stage technologies.³³ However, many of these technologies lack robustness or ease-of-use in the field and are usable for a single disease application only.³³

Here we introduce robust chemical methods and a simple instrument to rapidly quantify a wide range of chemical and microbial contaminations. We employed far-field optical detection, which is particularly practical because it does not require physical contact with the sample. Instead of using a commercial spectrophotometer, we developed a low-cost detection device to perform our tests (see the Supporting Information). The device achieves robustness and high sensitivity by concurrently detecting UV absorption and fluorescence. The use of an optical readout allows it to be applicable for the detection of a range of analytes. In this paper, we focus on the enzyme- and dye-based methods to quantify the concentration of several chemical contaminants and microbial pathogens in a wide range of household products, medicines, foods, and blood components.

Received: February 25, 2012

Revised: May 22, 2012

Accepted: May 27, 2012

Published: May 28, 2012

We developed or procured assays for detecting different poisons shown in Table 1. These have been known to appear at

Table 1. Applications for Detecting Poisons, Contaminants, and Pathogens and Their Detection Mechanisms

contaminant	contaminated materials	detection mechanism	spectral range
ethylene glycol	consumer household products and medicines	enzymatic	UV
diethylene glycol	consumer household products and medicines	enzymatic	fluorescence + UV
alcohols	groundwater	enzymatic	fluorescence + UV
food pathogens	foods, e.g., milk, eggs, cider	DNA dye	fluorescence
environmental pathogens	(recreational) water	DNA dye	fluorescence
bloodborne pathogens	blood	DNA dye	fluorescence

all levels above those deemed safe by the U.S. FDA and the European Community.^{10,28} We also measured the concentration of a range of primary alcohols in water, as alcohol in groundwater is a sign of gasoline spills or leaks. In addition, using DNA intercalator dyes, we measured the concentration of pathogenic microorganisms in common food materials that ordinarily contain little DNA, including *Salmonella* in egg white, *E. coli* in milk, and *V. cholera* in water, at levels known to cause symptoms. Finally, we used yeast with a genome size comparable to that of *Plasmodium* and quantified its concentration in a hematocyte suspension, as a rudimentary model for the detection of blood parasites, such as malaria. It is essential that the assays used work equally well on a range of household products without background noise causing false readings. To compensate for background noise, we tested two samples.

MATERIALS AND METHODS

Instrumentation. For detection, we used a detection device made from a rapid manufactured plastic housing that encases simple LEDs and detectors that surround the sample. Detection robustness was achieved by concurrently using UV absorption and fluorescence, as shown in Figure 1 and in the Supporting Information. This detector employs a round geometry allowing simultaneous multichannel measurement of a baseline and unknown contaminated sample held in standard glass test tubes that cost a few cents each. The detector uses a particularly narrow range of wavelengths relevant to the chemistry one wants to control. For our UV illumination source we chose single-color LEDs in this case, one with an emission peak at 365 nm, in the middle of a broad NADH absorption. For fluorescence illumination we chose a single-color green LED to detect the Amplex Ultrared (Invitrogen) fluorescence. The device had a sensitivity comparable to that of a commercial plate reader, as was tested by comparing the fluorescence emission from a standard glucose assay in both the device and a commercial plate reader (see the Supporting Information). Our detection method was based on comparing sensor output from two samples: one baseline sample made with a known amount of contaminant was held in a 6.5 mm diameter test tube (Durham Culture Tubes 6.50), and one unknown contaminated sample was prepared with an assay or dye and held in a second tube.

Chemical Methods. More detailed chemical methods and protocols may be found in the Supporting Information.

Ethylene Glycol. Samples (S) containing ethylene glycol (obtained from Sigma Aldrich SAJ first grade) were mixed with household products and medicines at different mass percentages (for details see the Supporting Information). To prepare the enzyme stock solutions, an alcohol dehydrogenase–NAD reagent (A) was made by adding 15 mL of Tris-HCl buffer, pH 8.8, and 0.1 M (Bio-Rad) to 50 mg of NAD (Sigma Aldrich N8535). In mixture B, 0.1 mL of Tris-HCl buffer, pH 8.8, and 0.1 M (Bio-Rad) were added to 100 mg of yeast alcohol dehydrogenase (USB/Affymetrix 10895). To start a sample reaction, 120 μ L of the sample (S) was placed in a round 6.50 mm glass tube (Durham Culture Tubes 6.50). Next an enzyme mixture (C) containing 480 μ L of solution B and 40 μ L of solution A was prepared. All volumes were confirmed by weighing with a scale

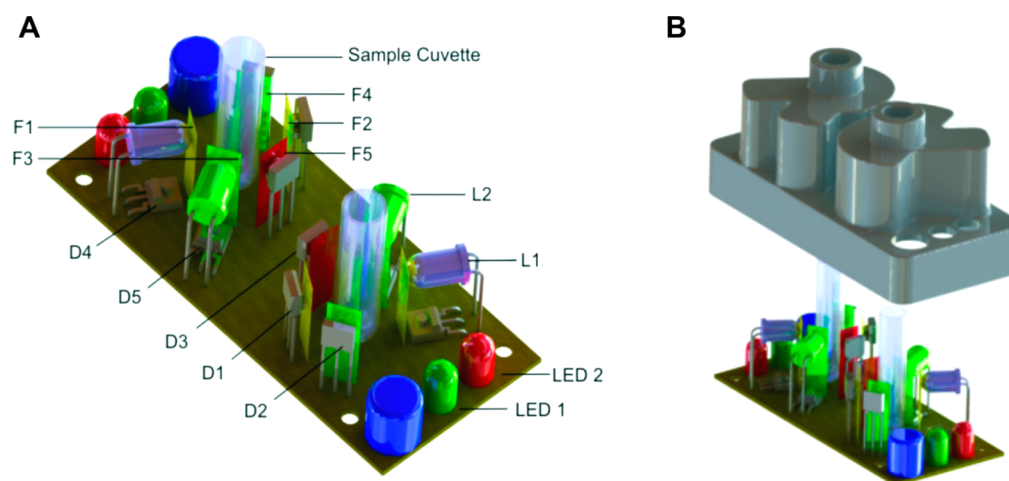


Figure 1. Schematic overview and rendering of our multichannel, multisample (baseline and prepared), UV–vis absorption and fluorescence detector. (A) Interior device electronics. UV light emitted by an LED (L1) passes through an excitation filter (F1), the sample, and another filter (F2) before absorption is detected (D1). Detector D4 provides a feedback signal to an op-amp that maintains constant light output from L1, the baseline level of which is set by a microcontroller. Light from a similarly stabilized green LED (L2) is filtered (F3) before passing through the sample. Green light is filtered and detected for green absorption (F4, D2) and red fluorescence (F5, D3). Voltage outputs from the detectors (D1, D2, D3) are digitized and sent from a microcontroller to an external computer. LED 1 (“yes”) and LED 2 (“no”) are simple light-readouts telling the end-user whether the sample is contaminated or not (LED 1 and LED 2 are design suggestions and have not been integrated into the used prototype). (B) To assemble a device, two mirror-image enclosure units are snapped together and placed over the circuit board containing the LEDs and detectors. The optical setup and electronics are precisely aligned in the enclosure by flexural springs molded into the cover, which force the components against reference features.

(Mettler Toledo). To start the reaction in our device, 240 μL of C was added to each tube containing sample (S). A 5.4 wt % EG sample in buffer was always run in parallel as a control.

Diethylene Glycol and Alcohols. Samples (S) of diethylene glycol and alcohols at different mass percentages were prepared in Tris-HCl buffer, pH 7.8, and 0.1 M (Bio-Rad). Stock solutions A and B (see above) were prepared. In addition, stock solutions of 0.05 wt % Amplex Ultrared in DMSO (solution D), 0.044 wt % horseradish peroxidase type 1 (Sigma Aldrich P8125) in Tris-HCl buffer, pH 7.8, 0.1 M (solution E), 12 wt % peroxidase from *Enterococcus faecalis* (Megazyme, EC 1.11.1.1) in phosphate buffer, pH 6.0, 0.1 M (solution F), and 0.2 mg/mL flavin adenin dinucleotide (Sigma Aldrich) in deionized water (solution G) were prepared. The final enzyme mixture H contained 480 μL of solution B, 40 μL of solution A, and 20 μL each of solutions D, E, F, and G. The reaction was started and read out as described for EG above. For the DEG samples, a reference sample of 5.4 wt % DEG and for alcohols a sample of 5.4×10^{-3} wt % were always run in the second chamber as a control.

Enzyme and pH Optimization. To screen different alcohol dehydrogenases for their specificity in reacting with DEG, we measured the fluorescence product in a plate reader (Molecular Devices) from our assay on 5.4 wt % EG samples in cough syrup and in glycerol, respectively. Pure buffer with one enzyme (USB) was used as a control. The “relative interference” of each enzyme was measured by dividing the initial fluorescence and UV reaction gradient of each sample by the control. The pH of the assay solution was optimized by varying the buffer pH from 6 to 9 and choosing the pH that gives the highest signal-to-noise ratio. The use of NADH oxidase instead of NADH peroxidase made the assay unstable, as NADH oxidase solution decays within minutes at room temperature (see the Supporting Information for more detailed methods).

***E. coli*, *Salmonella*, *V. cholera* Bacteria in Foods and Water.** We grew cultures of *E. coli* (strain DH5 α), (*Salmonella* strain LT2 Delta PhoP/Q S typhi), and *V. cholera* (strain VC O395NT). Bacteria were stained with 2.5 μM Syto 85 (Invitrogen catalog no. S11366) in deionized water for 3–30 min at 250 rpm and 30 $^{\circ}\text{C}$ in the dark; the resulting solutions of stained bacteria are referred to as samples I. The concentration of bacteria in each solution I was measured using the absorption value at 600 nm (Nanodrop 2000). We also stained samples of water (J), milk (K), and egg whites (L) with 2.5 μM Syto 85. Water (J) and milk (K) samples were stained directly as described above. Egg whites (L) were first diluted at a volume ratio of 1:1 with deionized water, then vortexed and filtered with a 100 μm filter (BD). The filtrate was centrifuged at 4300 rpm for 5 min, and the pellet was reconstituted with water at the same volume of the original egg white sample (L). We now prepared mixtures (M) of stained bacteria (I) with the respective stained products (J, K, and L) at different mass fractions. Mass fractions were determined using a scale (Mettler Toledo). To optically measure M using our detectors, 360 μL of a stained sample mixture M was placed in a round 6.50 mm glass tube (Durham Culture Tubes 6.50). All volumes were confirmed by weighing the samples (Mettler Toledo). A negative, buffer-only control was run in parallel and measured in the detectors. For Sytox Orange staining, cells were lysed using CellLytic (Sigma Aldrich) reagents and stained with 0.1 μM Sytox Orange (Invitrogen catalog no. S-34861) in TE buffer for 5 min. Further protocols are described in the Supporting Information, particularly those used for the dye optimization procedure.

Yeast in Red Blood Cells (Malaria Model). Baker's yeast (2.86 Mio yeast cells/mL in distilled water) was stained with 5 μM Syto 85 (Invitrogen catalog no. S11366) in deionized water for 5–60 min in the dark. After centrifugation, the bacteria were reconstituted with an equivolume amount of water in 0.5 g/mL sucrose (yielding solution N). The concentration of bacteria of the resulting solution (N) was measured using the absorption value at 600 nm (Nanodrop 2000). The same procedure was used to stain 2.86 Mio cells/mL bovine red blood cells (Lampire Biologicals 7240807) in sucrose–water, yielding stained solution O. After cell staining, mixtures P containing the components N and O at different mass fractions were prepared utilizing a scale (Mettler Toledo). For the measurement in our device,

360 μL of a stained sample mixture P (prepared above) was placed in a round 6.50 mm glass tube (Durham Culture Tubes 6.50). The volumes were confirmed by weighing the samples (Mettler Toledo). A negative, buffer-only control was run in parallel. For Sytox Orange staining, cells were lysed using CellLytic (Sigma Aldrich) reagents (see the Supporting Information) and stained with 0.1 μM Sytox Orange (Invitrogen catalog no. S-34861) in TE buffer for 5 min. Further protocols are described in the Supporting Information, particularly those used for the dye optimization procedure.

RESULTS AND DISCUSSION

Ethylene Glycol. Many reactions involving EG are known; however, those involving enzymes are particularly promising because they offer great specificity and sensitivity. To detect EG, we therefore chose a known, naturally occurring enzymatic reaction by which ADH converts a hydroxyl group to an aldehyde and simultaneously converts the coenzyme NAD^+ into NADH^5 (Figure 2A).³⁷ Hence, the absorption of NADH at 350–370 nm should reflect the concentration of EG.

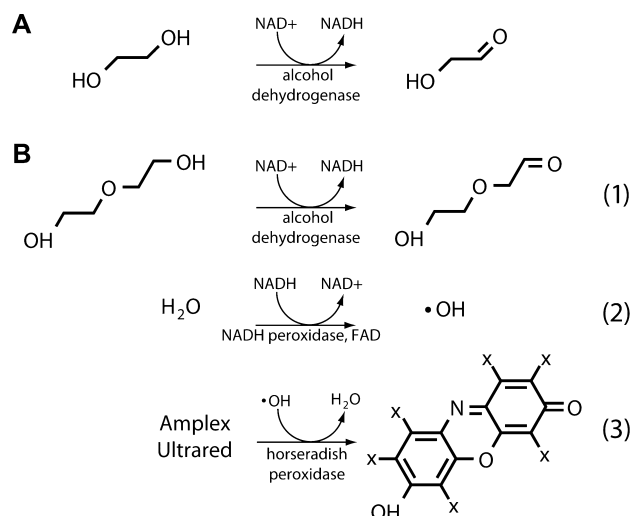


Figure 2. Chemical reactions. (A) ADH converts EG to an aldehyde in the presence of NAD^+ , which is converted to NADH ; we measured the increase in NADH concentration with our UV absorption detector. (B) The DEG reaction begins with the same first step (A), but instead of detecting NADH directly, NADH peroxidase converts NADH back to NAD^+ with an FAD coenzyme. This reaction generates hydrogen peroxide, which forms radicals that convert a resazurin-based dye into its fluorescent form. We detected the increase in fluorophore concentration with our fluorescence detector.

We illuminated the EG sample with the UV LED and measured the intensity change after the UV light had passed through the liquid EG sample, using a semiconductor light-to-voltage detector, as shown in the schematic in Figure 1B. To determine c_e , the mass fraction (concentration) of EG, we added a solution of ADH to the sample, inserted the sample into the sample chamber, and recorded the voltage $V_{\text{ua}}(t, c_e)$ measured by the UV absorption detector once per second for 5 min (see the Supporting Information and Materials and Methods). For pure EG ($c_e = 1$), the $V_{\text{ua}}(t, c_e)$ data fall on a straight line when plotted on a log–log plot, demonstrating a power-law behavior, as shown by the black circles in Figure 3A. Because the test tube has a circular cross section and the LED has a distribution of illumination angles, a single path length was not well-defined. Therefore, we could not rely on a simple Beer's law calculation for the absolute absorbance. Instead, we

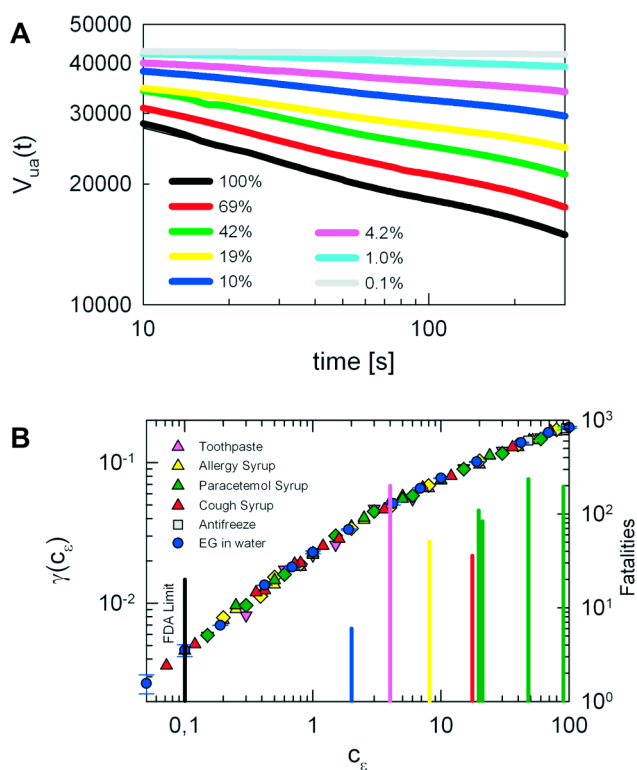


Figure 3. Detection of ethylene glycol contamination using UV absorption. (A) Time evolution of output voltage $V_{ua}(t)$ from the UV detectors, digitized as 16-bit integer, is shown on a log–log plot with symbols for different EG concentrations c_e in water. The data fall onto a straight line for each sample, demonstrating power-law scaling. (B) The magnitude of the slope of each line $\gamma(c_e)$ varies monotonically with c_e , shown with blue circles for pure EG. The $\gamma(c_e)$ values for a variety of different household products (colored triangles) and antifreeze (squares) all fall onto the same master curve, shown in black as a guide to the eye, demonstrating a universal scaling of this measure of EG concentration, irrespective of product contaminated. FDA safety limit $c_e = 10^{-3}$ is indicated with a black vertical line. EG concentrations of historical epidemics are indicated with bars, the color of which indicates the type of product contaminated, following the same color scheme as the data points; the number of deaths in each incident is represented by the height of the bar, indicated on the right-hand vertical axis.

calibrated the device with samples of known c_e in water, from the FDA safety limit of $c_e = 10^{-3}$ to $c_e = 1$.²⁸ In all cases we observed lines on the log–log plot, $V_{ua}(t, c_e) \sim t^{-\gamma(c_e)}$, as shown with colored symbols in Figure 3A. The power-law exponent magnitudes $\gamma(c_e)$ monotonically increased with c_e , as shown with the blue circles in Figure 3B. An optical feedback loop ensured that the LED intensity remained constant irrespective of environmental changes. Thus, there are no adjustable parameters in our determination of $\gamma(c_e)$. These data demonstrate our ability to measure c_e in drinking water with a detection limit below 0.1 wt % EG, which has caused sickness and death even in the United States,¹² at all concentrations deemed unsafe by the FDA.

Quantifying c_e in water, however, does not itself demonstrate the effectiveness of our detection methods in real-world ingestible products and medicines. These have a number of other ingredients that could interfere with the reaction. In particular, most products involved in historical EG poisoning incidents normally have a large fraction of glycerol, propylene glycol, or polyethylene glycol.^{6,10} These three-carbon glycols

have hydroxyl groups that ADH could, in principle, act upon, altering the measured reaction rate and obscuring the true c_e . There are a number of ADH variants commercially available. Although in general they give similar results for c_e in water, subtle differences in structure could have a greater impact on their relative sensitivity to EG in the presence of other glycols. We expected this sensitivity to be even more relevant for DEG (see below), as it is less reactive than EG due to its longer carbon chain. We hypothesized that we could screen the relative interference from glycols in different ADHs. This would allow us to pick the ADH with the least interference from glycols compared with DEG. To investigate the effects of these differences, we screened five different ADH variants for interference by mixing DEG with glycerol and, separately, with a mixture containing polyethylene glycol. We then compared the results of the DEG assay described below to the same concentration of DEG in water (see Table 8 in the Supporting Information). For our assay we selected the particular ADH variant (USB/Affymetrix) that exhibited the least interference, and we used it in all subsequent measurements.

Using the optimized ADH reaction we detected EG in real-world scenarios, namely, household products containing glycols (see Figure 3B). We measured samples with different c_e in a variety of unmodified ingestible household products, where contamination has led to historical poisonings that resulted in fatalities: toothpaste, cough syrup, acetaminophen/paracetamol syrup, and antihistamine (allergy) syrup.¹⁰ We chose several name brands and generics of each type, to ensure a broad sampling, and repeated the measurements in the same way as for water. Using the optimized ADH assay we found that $\gamma(c_e)$ increases monotonically with c_e , as in the pure case shown in Figure 3A. We also observed that the numerical values of $\gamma(c_e)$ remain consistent irrespective of the product tested, as shown with colored symbols in Figure 3B. Each data point is the result of a single measurement. We observed that all data from all products collapse onto a single master curve (with a standard error of 2.58%), which we indicate with a black line in the figure. By optimizing the ADH enzyme variants, we removed any interference from other glycols normally present in the products. This enabled us to achieve universal scaling, with no free-fitting parameters, for all products. Our enzyme method can quantify c_e at all unsafe levels above the FDA limit of 0.1 wt %, in all real products involved in historical contamination incidents. Our results furthermore suggest that the method could work well even in products in which EG contamination has not yet been observed.

Diethylene Glycol. Like EG, DEG poisoning has also killed thousands.^{4–21} We therefore repeated the ADH measurements for different DEG concentrations c_δ in water, expecting it to be less reactive because of the longer carbon chain of DEG compared to EG. Experimentally, we observed DEG to have significantly lower ADH activity, so that we could not distinguish low concentrations of DEG with this simple UV absorption assay alone. We therefore decided to amplify the DEG reaction products by adding enzymatic steps involving fluorescence-based dyes. Fluorescent dyes principally should have a higher signal-to-noise ratio than absorption. Beginning with the ADH reaction, we hence reacted the NADH product with NADH peroxidase and FAD, which generates free radicals that, in the presence of horseradish peroxidase, converts an essentially nonfluorescent resazurin-based dye into a resorufin-based fluorophore,³⁸ as shown in Figure 1B. However, the pH

for maximum activity differs significantly for the different components in the reaction chain: ADH is most active at $\text{pH} \geq 8$; NADH peroxidase at $\text{pH} 5$; HRP at $\text{pH} 6\text{--}6.5$; and NAD and FAD at $\text{pH} 7$. It was therefore not obvious that these particular steps could be coupled at a single fixed pH and still result in detectable fluorophore generation. We investigated this possibility by running the complete reaction chain under a variety of pH conditions (Figure 5A). We found the greatest amount of activity at $\text{pH} 7.8$, which we used for all subsequent measurements. We used NADH peroxidase, rather than NADH oxidase, as the latter solution is unstable and decays within minutes at room temperature (see the Supporting Information).

Under the optimized assay conditions, a $c_\delta = 1$ sample produced a visible red color change in a few minutes, whereas a $c_\delta = 0$ did not. This result demonstrated, at least qualitatively, the success of the reaction chain in the presence of DEG.

To more precisely quantify the progress of this reaction, we added a green LED spaced 60° from the UV LED for excitation, and two additional light detectors, using differently colored theater gel plastic to filter the green absorption and red fluorescence, were placed at 180° and 60° , respectively, relative to the green LED. The round geometry of the sample chamber, as well as offsetting the UV and fluorescence LED activation, made this addition possible, without interfering with the existing UV detection scheme. We could thus measure absorption and fluorescence with two excitation wavelengths, which is not possible with a common square cuvette geometry traditionally found in laboratory fluorimeters and spectrophotometers.

To measure c_δ in water, we mixed the enzymes and dye into the sample and immediately collected voltage data over time from the green and red fluorescence detector, $V_{\text{gf}}(t, c_\delta)$. As the reaction proceeded, the increase in fluorescence was manifested as an increase in $V_{\text{gf}}(t, c_\delta)$. These data fall onto a straight line when plotted on a semilog plot, demonstrating the exponential functional form $V_{\text{gf}}(t, c_\delta) \sim e^{\nu(c_\delta)t}$ as shown in Figure 4A. We found that the slope of this line, $\nu(c_\delta)$, increases monotonically with c_δ . However, our reaction involves the coupling of three enzymes and a dye, all of which may have slight variations in activity due to environmental factors, which could significantly influence $\nu(c_\delta)$. To account for these variations, we utilized the second, identical sample chamber of the sensor to simultaneously run a 100% DEG sample as a standard reference. Using $\nu_\delta^1 \equiv \nu(c_\delta = 1)$, as a normalization constant, we used the normalized $\nu'(c_\delta) = \nu(c_\delta)/\nu_\delta^1$ to account partially for the effects of variation in total enzyme activity. Furthermore, while collecting $V_{\text{gf}}(t, c_\delta)$, the device also collected $V_{\text{ua}}(t, c_\delta)$ automatically. These UV data should be sensitive only to the activity of the ADH. Therefore, we calculated the quantity $\gamma'(c_\delta) \equiv \gamma(c_\delta)/\gamma(c_\delta = 1)$, which provides a correction for the variations in absolute ADH activity. Combining the fitted data from the UV- and green-illuminated channels, we observed that $\nu'(c_\delta)\gamma'(c_\delta)$ rises monotonically with c_δ for DEG in water at all $c_\delta > 0.001$, the FDA safety limit, as shown in Figure 4B. Each data point in Figure 4B is the result of at least three independent runs, the percentage errors of which decrease with increasing c_δ . The percentage errors are on average 10%, and as low as 3.1% for $c_\delta = 0.25$. As in the EG case, we repeated the measurements for DEG in various household products: once again, we found that the data for some products collapse onto a single curve, although with slightly more scatter than in the EG case, as shown in Figure 4B. The scatter at each data point decreases

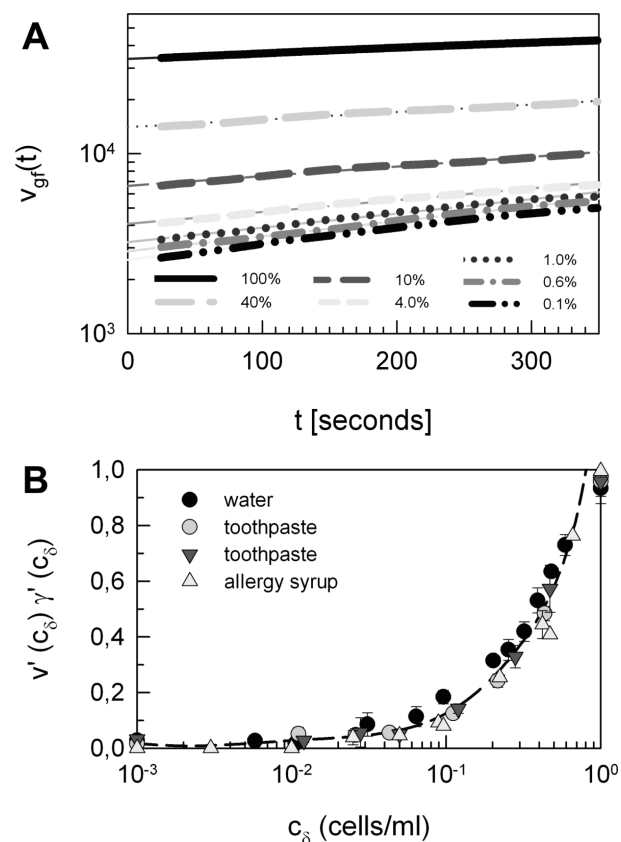


Figure 4. Detection of diethylene glycol using a combination of green→red fluorescence and UV absorption. (A) Time evolution of output voltage $V_{\text{gf}}(t)$ from the green→red fluorescence detector, digitized as 16-bit integer, is shown on a semilog plot with symbols for different DEG concentrations in water; the data fall onto a straight line for each sample, indicating exponential behavior. (B) Combination of normalized UV absorption and green→red fluorescence data, $\nu'(c_\delta)\gamma'(c_\delta)$, is shown with solid black circles for DEG in water; data for other ingestible household products (other symbols) fall on the same master curve (dashed line).

from 33 to 1.5% as c_δ increases from 0.001 to 1. These data demonstrate our ability to detect DEG, just as for EG, in several ingestible household products and medicines.

The ability to detect these contaminants in remote areas would be greatly enhanced if the chemistry were stable without refrigeration. Indeed, the enzymes and dyes we used are packaged in dry, lyophilized form and can be shipped overnight without temperature control. How long the activities of these components remain consistent, however, is not well characterized. To test the longer term stability of our assays, we created large samples with $c_\delta = 0.10$ and $c_e = 0.10$ and, over the course of several weeks, left all samples, and lyophilized enzymes and dyes, at room temperature, without any temperature control. For each measurement, we made a new enzyme solution and ran the EG and DEG assays. Strikingly, in all cases, the absolute variation in the measured glycol concentrations was $< \pm 1\%$, even as the enzymes were at room temperature for > 3 weeks, as shown in Figure 5B. These data demonstrate that our approach to normalizing variations by a combination of LED output stabilization, calibration with reference samples at known concentrations, and combining data from multiple channels allowed us to eliminate any changes in enzyme activity within our measurement un-

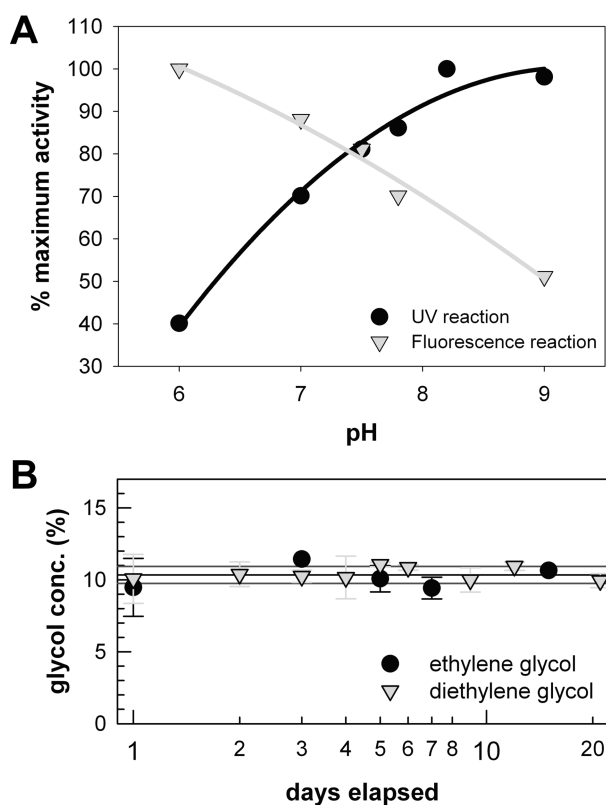


Figure 5. (A) pH optimization of the DEG assay: by varying the buffer pH from 6 to 9 we observe the highest overall signal-to-noise levels between pH 7.5 and 8, at which both fluorescence absorptions are at a high percentage of their maximum activity. (B) Assay stability measurement using the same $c_\delta = 0.1$ (DEG) and $c_e = 0.1$ (EG) samples over time, with enzymes left to sit at room temperature. Average and standard deviation of measurements are marked with black and grey lines, respectively. In all cases, the measured glycol concentrations remained stable to within $\pm 1\%$ throughout the course of >3 weeks.

certainty. Consequently, our device and chemistry are accurate without requiring a continuous chain of refrigeration (which, for example, is required for immunoassays and other sensitive biochemistry) or other infrastructure, and therefore may be suitable for deployment in disaster areas.

Alcohols. We used ADH to detect glycols that have multiple hydroxyl groups; however, the enzyme originally evolved to convert simple alcohols, with a single hydroxyl group. ADH reacts far more rapidly with alcohols, which suggests our assay might detect alcohols at far lower concentrations c_α . To test this hypothesis, we ran our assay on several alcohols mixed with buffer, including ethanol, 1-propanol, 2-propanol, 1-butanol, 1-pentanol, 1-hexanol, 1-heptanol, and 1-octanol. As for the DEG measurement, we calculated γ' and ν' from the UV- and green-illuminated channels, but used $c_\alpha = 0.01$ as the reference concentration for each alcohol (instead of $c_\delta = 1$, in the case of DEG). Each data point is the result of at least three independent runs. We observed that the $\gamma'(c_\alpha)\nu'(c_\alpha)$ data for all primary alcohols collapse onto a single master curve, for all c_α above the part per billion (ppb) level, as shown in Figure 6A. The average percentage error between different alcohols at a certain concentration is as low as 7.5% at $c_\alpha = 0.001$. Furthermore, for $c_\alpha = 0.01$, the $\gamma'(0.01)\nu'(0.01)$ data for primary alcohols decrease monotonically with the alcohol carbon number and

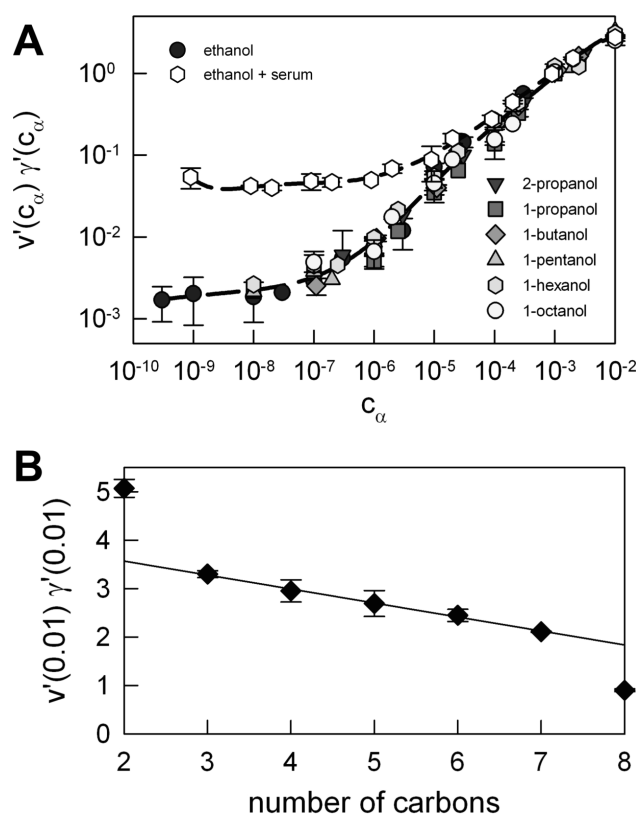


Figure 6. Detection and characterization of alcohols. (A) Combination of normalized UV absorption and green-to-red fluorescence data, $\nu'(c_\alpha)\gamma'(c_\alpha)$, for various alcohols in water, is shown as a function of concentration c_α . The data collapse onto a single master curve, marked with a black curve, for all concentrations greater than a few parts per billion. Data for ethanol in blood serum plateaus to a background of a few parts per million, well below the legal blood-alcohol limits in a variety of countries, which range from 2×10^{-4} to 8×10^{-4} . (B) The absolute value of $\nu'(0.01)\gamma'(0.01)$ for primary alcohols decreases monotonically with increasing carbon number. For alcohols with 3–7 carbons, this decrease is linear, marked with a solid line.

are nearly linear within the range of 3 (propanol) to 7 (hexanol) carbons (Figure 6B). These data demonstrate how our device and chemistry may provide an extremely sensitive probe for the presence of alcohols, and, for some primary alcohols, allow them to be identified when concentration is known. For example, this test could be used to detect alcohol in groundwater, which is a sign of gasoline spills or leaks. In addition, we repeated the measurement of ethanol in blood serum, as a way to measure blood-alcohol content, shown with hexagons in Figure 6A. Each data point in Figure 6 is the result of at least three independent runs. These data overlap the other alcohols exactly for $\gamma'(c_\alpha > 10^{-6})$. We can therefore quantify accurately the c_α for ethanol in blood serum 2 orders of magnitude below the standard drunk-driving limits of $c_\alpha = (2-8) \times 10^{-4}$. This method may provide another avenue for rapid, low-cost, blood-alcohol measurement in the field, with substantially greater accuracy than breath-based tests.

Food and Environmental Pathogens. The ability to detect transmission and fluorescence from two excitation wavelengths simultaneously allows us to detect a broad range of other chemical reactions or interactions that generate a change in optical activity. For example, we could detect DNA with low-cost intercalator dyes, known to be stable at room temperature for months. This suggested a new use for our

system, the detection of microbial DNA, which implies the presence of its host organism, in materials where no DNA should be found, such as recreational water and many foods, where contamination has led to lethal epidemics. To test our ability to detect such microbial contamination, we mixed different microbial concentrations c_μ of *V. cholera*, *Salmonella*, and *E. coli* bacteria in water, added a DNA intercalator dye, removed free dye, and then measured the final, static green–red fluorescence intensity $V_{gf}^\infty(c_\mu) \equiv V_{gf}^\infty(t \rightarrow \infty, c_\mu)$. The total preparation and measurement time was only a few minutes. In both cases, we found that $V_{gf}^\infty(c_\mu)$ rises with $c_\mu > 10^5$ CFU/mL (CFU = colony-forming units), with a readily discernible detection limit of 10^6 CFU/mL (based on Kaiser's criterion, see the Supporting Information). Our minimum detectable c_μ is comparable to total organism concentrations detected in several historical epidemics.^{39,40} Furthermore, we tested the concentration of pathogens in pond water (Bow, NH) and measured a baseline activity indistinguishable from background levels in doubly distilled water. These data demonstrate the utility of our method to potentially preventing recreational water epidemics, when fast turn-around times may be desirable. Even though the methods introduced here can detect bacteria at concentrations found in several historical epidemics,^{39,40} lower detection limits may be desirable because the presence of as low as 10 cells of *Salmonella* or *E. coli* O157:H7 may be an infectious dose.⁴¹ The EPA recommendation for recreational waters is around 1 CFU/mL,⁴² even though higher detection limits may be acceptable, especially when fast turn-around times are needed. To increase detection sensitivity, we optimized the fluorescent dyes and used lysed cells rather than whole cells, where the DNA is expected to be more accessible to the dyes. As shown in Figure 8 we achieved a readily discernible detection limit of $c_\mu = 10^4$ CFU/mL (based on Kaiser's criterion) by lysing the cells and using the DNA dye Sytox Orange rather than Syto 85. Sytox Orange was chosen, as it is compatible with the current optical setup of the device. Further optimization of dyes and lysis conditions could improve this detection limit even more (see the Supporting Information, part G).

Another major area where DNA should not be present is in foods that do not contain cellular tissue from animals or plants. Many of these, such as milk and eggs, have been involved in massive food poisoning outbreaks when contaminated by bacteria such as *E. coli* or *Salmonella*.^{22,25} Unlike drinking water, however, these complex biological materials contain other components with the potential to interfere with the DNA intercalator dyes. To test our ability to quantify microbial contamination in these materials, we repeated the above procedure with *E. coli* in milk and *Salmonella* in egg white, combinations that have caused lethal food poisonings in the past. Once again, in both cases, $V_{gf}^\infty(c_\mu)$ rose with c_μ . However, the curves of $V_{gf}^\infty(c_\mu)$ for the four bacterial data sets did not overlap on the same curve, possibly due to differences in autofluorescence of the materials and foods. With a traditional fluorometer, little could be done without further sample modifications. The multichannel design of our detector, however, gave us a number of additional options, because we also collected automatically the final, static green absorption $V_{gf}^\infty(c_\mu)$ and UV→ red fluorescence $V_{uf}^\infty(c_\mu)$. We searched for combinations of channel metrics for which all four bacteria collapsed onto the same master curve. By trial, we found universal data collapse for the normalized multichannel metric $V_{gf}^\infty(c_\mu)((V_{uf}^\infty(c_\mu) \cdot V_{ga}^\infty(c_\mu)))^{1/2}$, as shown in Figure 7A. Again, using Syto 85 we found that $V_{gf}^\infty(c_\mu)((V_{uf}^\infty(c_\mu) \cdot V_{ga}^\infty(c_\mu)))^{1/2}$ rises

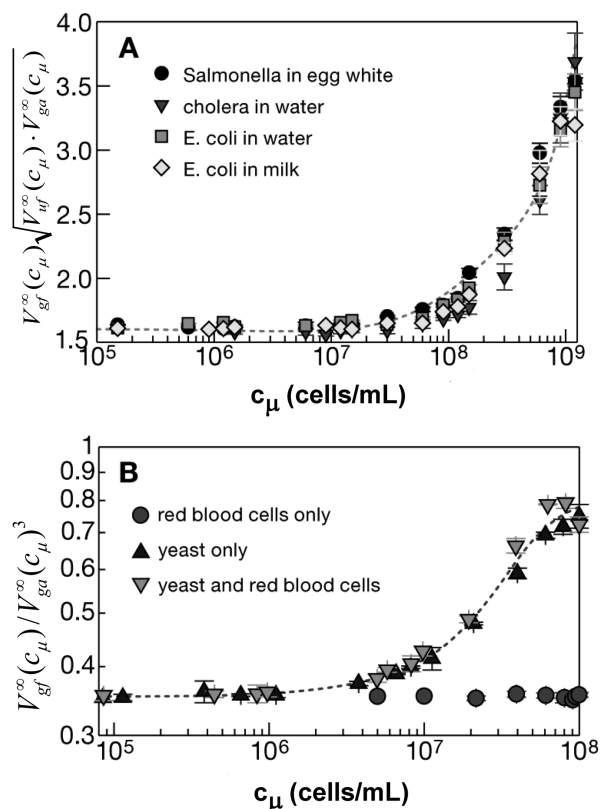


Figure 7. Detection of microbial contamination. (A) Combined normalized multichannel data $V_{gf}^\infty(c_\mu)((V_{uf}^\infty(c_\mu) \cdot V_{ga}^\infty(c_\mu)))^{1/2}$ from DNA intercalator dye in the presence of prokaryotic pathogens at different concentrations c_μ . In all cases, the data from *V. cholera* in water, *E. coli* in water and in milk, and *Salmonella* in egg white all collapse onto the same master curve (dotted line). This demonstrates universal, species-independent behavior of our bacterial detection scheme. (B) Rudimentary model for the detection of eukaryotic blood parasites, such as malaria. Combined normalized multichannel data $V_{gf}^\infty(c_\mu) / V_{ga}^\infty(c_\mu)^3$ for dyed yeast both in water (black triangles) and in red blood cells (inverted gray triangles) scale onto the same master curve (dotted line), and at low concentration plateau to the background sample of red blood cells alone (circles).

with $c_\mu > 10^5$ CFU/mL, with a readily discernible detection limit of 10^6 CFU/mL (Kaiser's criterion). Given the similar spectral characteristics, we expect that using Sytox Orange would further reduce the detection limit to $c_\mu \sim 10^4$ CFU/mL as in the case of pure bacteria shown in Figure 8.

These data demonstrate how our device can be used in a general way to measure microbial concentration in substrates that should not contain DNA, irrespective of particular bacteria or substrate. This is particularly important in foods and medicines, in which a wide range of bacteria are known to cause poisoning.^{25,26} We emphasize that our measurements were taken directly on samples and require only a few minutes of dye exposure. Our results were unchanged over various dye incubation times from 3 to 30 min (see the Supporting Information), in contrast to the hours or days required for culturing or PCR analysis.³⁶ Our detection limit of 10^4 CFU/mL is comparable to most electrical, electrochemical (e.g., impedance, DEP), and immunochemical biosensors, which usually have detection limits between 10^3 and 10^5 CFU/mL with an assay time of at least 2 h under ideal conditions.^{43–47} Other optical methods (e.g., SPR, IR, optical fibers, etc.) may achieve even lower detection limits, but often require several

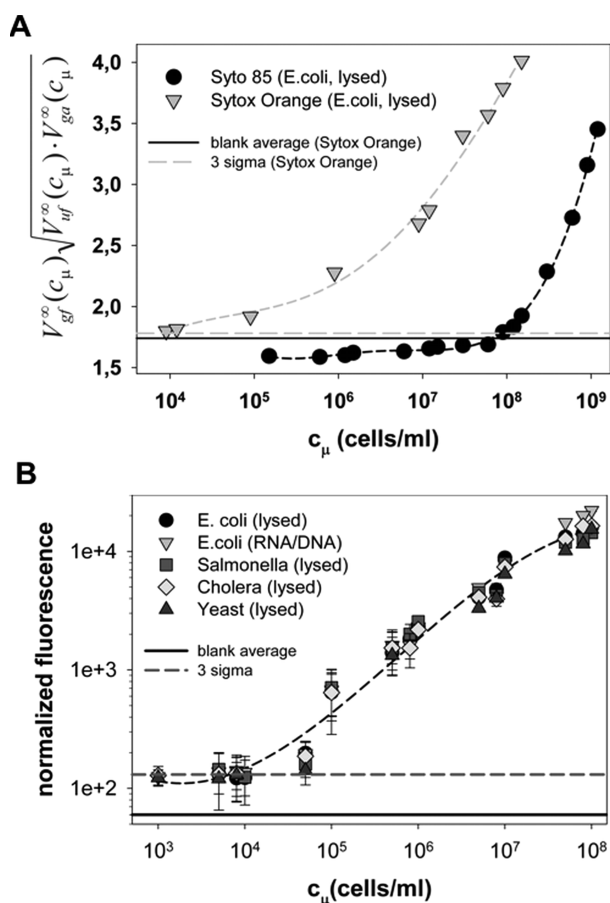


Figure 8. Dye optimization. (A) Comparison of Sytox Orange and Syto 85 detection limits. Shown are the combined normalized multichannel data $V_{gf}^{\infty}(c_{\mu}) \sqrt{V_{uf}^{\infty}(c_{\mu}) \cdot V_{ga}^{\infty}(c_{\mu})}$ from DNA intercalator dyes in the presence of *E. coli* cells at different concentrations c_{μ} . Using Sytox Orange with lysed *E. coli* cells improves the detection limit to $c_{\mu} = 10^4$ CFU/mL, compared with 10^6 CFU/mL in Syto 85. (B) Validation of Sytox Orange staining for different bacteria (*Salmonella*, *V. cholera*, *E. coli*) and yeast. This graph shows Sytox Orange stained lysed bacteria and lysed yeast cells at different concentrations measured in a plate reader (the sensitivity of which is comparable to the used device, see the Supporting Information). The fluorescence values are normalized by the pathogen genome size and are the averages of three independent runs. A detection limit of $c_{\mu} = 10^4$ CFU/mL (based on Kaiser's 3δ criterion) was achieved for all bacteria, demonstrating that Sytox Orange will improve the detection limit for all tested pathogens.

hours⁴³ and/or cost around 2 orders of magnitude more than the sensor described here.^{41,48} Traditional methods (such as cell culture, PCR, or ELISAs) have lower detection limits between 10^1 and 10^6 CFU/mL. However, they require incubation of several hours (PCR 4–6 h) to days (culture methods up to 5–7 days), as well as a stable laboratory environment often in combination with expensive equipment.⁴¹ The introduced detection scheme may therefore be used as a simple, low-cost, first screen and line of defense for pathogen contamination in a range of consumer products, recreational water, medicines, and food products.

Bloodborne Pathogens (e.g. Malaria). In addition to prokaryotes, we could apply the same method to a eukaryotic biological system in which the presence of DNA indicates the presence of pathogenic microbial invasion. Several bloodborne pathogens, for example, malaria-causing plasmodium, invade

red blood cells (RBCs), which have no DNA of their own. Moreover, RBCs can be separated from other DNA-bearing cells in blood using existing low-cost methods.⁴⁹ It might thus be possible for our methodology to detect this type of parasitic blood infection. To test this concept qualitatively, we created a rudimentary model for malarial invasion by dyeing suspensions of yeast with Syto 85, which we chose because they are safe to handle and have a total genome size about half that of plasmodium. We dyed yeast both in water and mixed with red blood cells as a model for malaria. After a brief incubation, we measured fluorescence and absorption, following the protocol as for bacteria. As in the bacterial case, when using fluorescence or absorption alone, different data sets scaled differently. In particular, the data for yeast in RBCs did not overlap that for yeast in water. We therefore combined the different parameters until we achieved universal data collapse. We found that, when normalizing the green→red fluorescence intensity by the cube of the green absorption, $V_{gf}^{\infty}(c_{\mu})/V_{ga}^{\infty}(c_{\mu})^3$, the data from both sets fell onto the same curve—and at low concentrations asymptote to the baseline value we measure for RBCs alone, as shown in Figure 7B. Again, using Syto 85 we found that $V_{gf}^{\infty}(c_{\mu})/V_{ga}^{\infty}(c_{\mu})^3$ rises with c_{μ} at a detection limit of $c_{\mu} > 8 \times 10^5$ CFU/mL (based on Kaiser's criterion). The detection limit could again be improved by using lysed cells and the DNA–dye Sytox Orange instead of Syto 85. We therefore stained pure, lysed yeast cells with Sytox Orange and achieved a detection limit of $c_{\mu} \sim 10^4$ CFU/mL as for the tested bacteria (see Figure 8B). These preliminary data demonstrate that the intercalator has no significant background interference from residual RNA or ribosomal nucleotides in the RBCs. Therefore, our method has the potential to quantify rapidly in RBC suspensions the concentration of bloodborne DNA-bearing parasites, such as plasmodium (malaria), trypanosoma (sleeping sickness and chagas), and the eggs of trematodes (schistosomiasis).

In this paper, contaminants were detected directly in various substances, without separation, purification, concentration, or incubation. New enzyme- and dye-based methods to detect (di)ethylene glycol in consumables above 0.1 wt % without interference and alcohols above 1 ppb were introduced. Using DNA intercalating dyes a range of pathogens in water, foods, and blood were detected without background signal at a detection limit of 10^4 CFU/mL. The detection scheme uses fluorescence and/or UV absorption measurements made on samples in a small round test tube. Our simple system makes practical the multiple channels and samples that allow us to normalize by references and combine data from different simultaneous measurements. The individual channels within our detector have sensitivities comparable to commercial optical laboratory instruments costing significantly more. In addition, contaminant concentrations we measured did not change with background substrate, which demonstrates that our detection methods are broadly effective in a wide variety of substances, and could apply in a general way to new substances where contamination might not yet have been found.

We emphasize that we have but scratched the surface of this exciting area, and our preliminary results can be improved and extended in many ways. We have examined a limited number of contaminants, but our strategy should be applicable to any chemical reaction that in the presence of a contaminant leads to a change in optical activity. For example, commercial kits are available that use a fluorescence-generating reaction to detect melamine in milk products.

The effective detection sensitivity of our scheme could be improved by dye optimization, concentration of microorganisms through mechanical methods such as filtering, or, when time is not a factor, incubation at elevated temperatures. The sensitivity could be further improved by adding a third LED or by optimizing LEDs, filter specifications, and excitation and emission times to the specific dye used. Moreover, for bacterial detection, we chose a nonspecific DNA intercalator dye because of its extremely low cost and high stability, but as a result our assay is insensitive to the actual genome being detected, and the sensitivity is limited. In many situations, when continuous refrigeration is available and cost pressure is not so severe, more specific biochemical tagging (e.g., molecular beacons), DNA amplification (isothermal or PCR), or immunoassays (e.g., antibodies, ELISAs) could be used to increase detection sensitivity and/or to detect the presence of specific, targeted pathogens.

Our chemistry is stable for weeks without refrigeration, and the rapid detection time of our assays allows testing of perishable foods and ingestible products, which often are not tested because current culturing-based methods require multiple days. The device we created is also robust and simple to use. In the future it could be run on batteries, and a smart mobile phone/tablet platform could be used to aggregate data for use in remote areas. One could also envisage a device consisting of LEDs or a simple number readout that gives the end-user a simple yes or no answer of whether the sample is contaminated (as indicated in Figure 1).

This new capability may have potential applications in much broader sampling of both domestic and imported foods and agricultural products, enabling end-to-end characterization within a food or medicine supply chain. By leveraging amplification methods and existing chemical labeling technologies to identify the presence of chemical and biological contaminants, we hope that our work might be a first step toward preventing many diseases and deaths.

■ ASSOCIATED CONTENT

● Supporting Information

Recent contamination incidents leading to sickness, hospitalization, and death and detailed Materials and Methods. This material is available free of charge via the Internet at <http://pubs.acs.org>.

■ AUTHOR INFORMATION

Corresponding Author

*E-mail: hoehl@mit.edu.

Funding

This work was supported by CIMIT, the Legatum Center at MIT, Robert Bosch GmbH, and Prof. Slocum's Pappalardo Chair discretionary funds.

Notes

The authors declare no competing financial interest.

■ ACKNOWLEDGMENTS

We thank the MIT Legatum Center, H. Ma, J. Voldman, the CR/ARY 2 team at Robert Bosch GmbH (particularly J. Steigert, B. Faltin, and P. Rothacher), S. Finch, L. Przybyła, M. Vahey, D. Markus, J. Helferich, and B. Stupak for their contributions and guidance.

■ ABBREVIATIONS USED

EG, ethylene glycol; DEG, diethylene glycol; ADH, alcohol dehydrogenase; NAD, nicotinamide adenine dinucleotide; FAD, flavin adenine dinucleotide; HRP, horseradish peroxidase; CFU, colony-forming units.

■ REFERENCES

- (1) U.S. House of Representatives Subcommittee on Science and Technology. 2007, FDA: Science and Mission at Risk, Report of the Subcommittee on Science and Technology, available at http://www.fda.gov/ohrms/dockets/ac/07/briefing/2007-4329b_02_01_FDA%20Report%20on%20Science%20and%20Technology.pdf (accessed May 20, 2011).
- (2) Sack, K.; Williams, T. Deaths of 9 Alabama patients tied to intravenous supplement. *N. Y. Times* **2011**, March 30.
- (3) Tagliabue, J. Scandal over poisoned wine embitters village in Austria. *N. Y. Times* **1985**, Aug 2.
- (4) Bogdanich, W.; Hooker, J. Toxic toothpaste made in China is found in the U.S. *N. Y. Times* **2007**, May 6.
- (5) Gomes, R.; Liteplo, R.; Meek, M. E. *Ethylene Glycol: Human Health Aspects*; World Health Organization: Geneva, Switzerland, 2002.
- (6) ATSDR (U.S. Department of Human Health and Services, Agency for Toxic Substances and Disease Registry). 2010, Toxicological Profile for Ethylene Glycol, available at <http://www.atsdr.cdc.gov/toxprofiles/tp96-c7.pdf> (accessed May 20, 2011).
- (7) Schep, L. J.; Slaughter, R. J.; Temple, W. A.; Beasley, D. M. G. Diethylene glycol poisoning. *Clin. Tox.* **2009**, *47* (6), 525–535.
- (8) Schier, J.; Conklin, L.; Sabogal, R.; Dell'Aglio, D.; Sanchez, C.; Sejvar, J. Medical toxicology and public health—update on research and activities at the centers for disease control and prevention and the agency for toxic substances and disease registry. *J. Med. Tox.* **2008**, *4* (1), 40–42.
- (9) Wax, P. M. Elixirs, diluents, and the passage of the 1938 Federal Food, Drug and Cosmetic Act. *Ann. Intern. Med.* **1995**, *122* (6), 456.
- (10) SCCP (European Commission Scientific Committee on Consumer Products). 2008, Opinion on Diethylene Glycol, available at http://ec.europa.eu/health/ph_risk/committees/04_sccp/docs/sccp_o_139.pdf (accessed May 20, 2011).
- (11) Leikin, J. B.; Toerne, T.; Burda, A.; McAllister, K.; Erickson, T. Summertime cluster of intentional ethylene glycol ingestions. *JAMA, J. Am. Med. Assoc.* **1997**, *278*, 1406.
- (12) Schultz, S.; Kinde, M.; Johnson, D. Ethylene glycol intoxication due to contamination of water systems. *Morb. Mortal. Wkly. Rep.* **1987**, *36*, 611–614.
- (13) U.S. Environmental Protection Agency. 2001, Potential Contamination Due to Cross-Connections and Backflow and the Associated Health Risks, Office of Ground Water, EPA Distribution System Issue Paper, available at http://www.epa.gov/ogwdw/disinfection/tcr/pdfs/issuepaper_tcr_crossconnection-backflow.pdf (accessed May 20, 2011).
- (14) Abubukar, A.; Awosanya, E.; Badaru, O.; Haladu, S.; Nguku, P.; Edwards, P.; Noe, R.; Teran-Maciver, M.; Wolkin, A.; Lewis, L. Fatal poisoning among young children from diethylene glycol-contaminated acetaminophen—Nigeria, 2008–2009. *Morb. Mortal. Wkly. Rep.* **2009**, *58* (48), 1345–1347.
- (15) Singh, J.; Dutta, A. K.; Khare, S.; Dubey, N. K.; Harit, A. K.; Jain, N. K.; Wadhwa, T. C.; Gupta, S. R.; Dhariwal, A. C.; Jain, D. C. Diethylene glycol poisoning in Gurgaon, India, 1998. *Bull. WHO* **2001**, *79*, 88–95.
- (16) O'Brien, K. L.; Selanikio, J. D.; Heedivert, C.; Placide, M. F.; Louis, M.; Barr, D. B.; Barr, J. R.; Hospedales, C. J.; Lewis, M. J.; Schwartz, B. Epidemic of pediatric deaths from acute renal failure caused by diethylene glycol poisoning. *Am. Med. Soc.* **1998**, *279* (15), 1175.
- (17) Hanif, M.; Mobarak, M. R.; Ronan, A.; Rahman, D.; Donovan, J. J., Jr.; Bennish, M. L. Fatal renal failure caused by diethylene glycol in

paracetamol elixir: the Bangladesh epidemic. *Br. Med. J.* **1995**, *311* (6997), 88.

(18) Okuonghae, H. O.; Ighogboja, I. S.; Lawson, J. O.; Nwana, E. J. Diethylene glycol poisoning in Nigerian children. *Ann. Trop. Paediatr.* **1992**, *12* (3), 235.

(19) Pandya, S. K. Letter from Bombay. An unmitigated tragedy. *Br. Med. J.* **1988**, *297* (6641), 117.

(20) Wax, P. M. It's happening again—another diethylene glycol mass poisoning. *Clin. Toxicol.* **1996**, *34* (5), 517–520.

(21) Osterberg, R. E.; See, N. A. Toxicity of excipients—a Food and Drug Administration perspective. *Int. J. Toxicol.* **2003**, *22* (5), 377.

(22) Scallan, E.; Hoekstra, R. M.; Angulo, F. J.; Tauxe, R. V.; Widdowson, M. A.; Roy, S. L.; Jones, J. L.; Griffin, P. M. Foodborne illness acquired in the United States—major pathogens. *Emerg. Infect. Dis.* **2011**, *17*, 7.

(23) CDC (Centers for Disease Control and Prevention). 2011, Salmonella Outbreaks, available at <http://www.cdc.gov/salmonella/outbreaks.html> (accessed May 20, 2011).

(24) CDC (Centers for Disease Control and Prevention). 2011, Outbreak Investigation of *E. coli*, available at <http://www.cdc.gov/ecoli/outbreaks.html> (accessed May 20, 2011).

(25) Mead, P. S.; Slutsker, L.; Dietz, V.; McCaig, L. F.; Bresee, J. S.; Shapiro, C.; Griffin, P. M.; Tauxe, R. V. Food-related illness and death in the United States. *Emerg. Infect. Dis.* **1999**, *5* (5), 607.

(26) Griffith, D. C.; Kelly-Hope, L. A.; Miller, M. A. Review of reported cholera outbreaks worldwide, 1995–2005. *Am. J. Trop. Med. Hyg.* **2006**, *75* (5), 973.

(27) Theron, J.; Cilliers, J.; Du Preez, M.; Brözel, V. S.; Venter, S. N. Detection of toxigenic *Vibrio cholerae* from environmental water samples by an enrichment broth cultivation—pit stop semi nested PCR procedure. *J. Appl. Microbiol.* **2000**, *89* (3), 539–546.

(28) U.S. Food and Drug Administration. 2010, Guidance for Industry: Testing of Glycerin for Diethylene Glycol, available at <http://www.fda.gov/downloads/Drugs/GuidanceComplianceRegulatoryInformation/Guidances/ucm070347.pdf> (accessed May 20, 2011).

(29) Leonard, P.; Hearty, S.; Brennan, J.; Dunne, L.; Quinn, J.; Chakraborty, T.; O'Kennedy, R. Advances in biosensors for detection of pathogens in food and water. *Enzyme Microb. Technol.* **2003**, *32* (1), 3–13.

(30) Nugen, S. R.; Baeumner, A. J. Trends and opportunities in food pathogen detection. *Anal. Bioanal. Chem.* **2008**, *391* (2), 451–454.

(31) Velusamy, V.; Arshak, K.; Korostynska, O.; Oliwa, K.; Adley, C. An overview of foodborne pathogen detection: in the perspective of biosensors. *Biotechnol. Adv.* **2010**, *28* (2), 232–254.

(32) Kenyon, A. S.; Shi, X.; Wang, Y. A. N. Simple, at-site detection of diethylene glycol/ethylene glycol contamination of glycerin and glycerin-based raw materials by thin-layer chromatography. *J. AOAC Int.* **1998**, *81* (1), 44–50.

(33) Yager, P.; Domingo, G. J.; Gerdes, J. Point-of-care diagnostics for global health. *Annu. Rev. Biomed. Eng.* **2008**, *10*, 107–144.

(34) Kost, G. J. Newdemics, public health, small-world networks, and point-of-care testing. *Point Care* **2006**, *5* (4), 138.

(35) Fukushima, H.; Tsunomori, Y.; Seki, R. Duplex real-time SYBR green PCR assays for detection of 17 species of food-or waterborne pathogens in stools. *J. Clin. Microbiol.* **2003**, *41* (11), 5134.

(36) Yasmin, M.; Kawasaki, S.; Kawamoto, S. Evaluation of multiplex PCR system for simultaneous detection of *Escherichia coli* O157:H7, *Listeria monocytogenes* and *Salmonella enteritidis* in shrimp samples. *Bangl. J. Microbiol.* **2008**, *24* (1), 42–46.

(37) Eckfeldt, J. H.; Light, R. T. Kinetic ethylene glycol assay with use of yeast alcohol dehydrogenase. *Clin. Chem.* **1980**, *26* (9), 1278.

(38) Batchelor, R. H.; Zhou, M. A resorufin-based fluorescent assay for quantifying NADH. *Anal. Biochem.* **2002**, *305* (1), 118.

(39) Gadgil, A. Low cost UV disinfection system for developing countries: field tests in South Africa. *Annu. Rev. Energy Environ. Fed.* **1998**, *23*, 253.

(40) Danley, A. A.; Watts, M. J. Installation of bio-sand filters in Petite Paradise, Haiti. *Proc. Water Environ. Fed.* **2009**, *12*, 3892–3897.

(41) Lazcka, O.; Del Campo, F.; Munoz, F. Pathogen detection: a perspective of traditional methods and biosensors. *Biosens. Bioelectron.* **2007**, *22*, 1205–1217.

(42) Noble, R.; Weisberg, S. A review of technologies for rapid detection of bacteria in recreational waters. *J. Water Health* **2005**, *3*, 381–392.

(43) Yan, L.; Bashir, L. Electrical/electrochemical impedance for rapid detection of foodborne pathogenic bacteria. *Biotechnol. Adv.* **2008**, *26*, 135–150.

(44) Ivnitsk, D.; Abdel-Hamid, I.; Atanasov, P.; Wilkins, E. Biosensors for detection of pathogenic bacteria. *Biosens. Bioelectron.* **1999**, *14*, 599–624.

(45) Ivnitsk, D.; Abdel-Hamid, I.; Atanasov, P.; Wilkins, E.; Stricker, S. Application of electrochemical biosensors for detection of food pathogenic bacteria. *Electroanalysis* **2000**, *12*, 317–325.

(46) Su, X. L.; Li, Y. A self-assembled monolayer-based piezoelectric immunosensor for rapid detection of *Escherichia coli* O157:H7. *Biosens. Bioelectron.* **2004**, *19* (6), 563–574.

(47) Rand, A. G.; Ye, J.; Brown, C. W.; Letcher, S. V. Optical biosensors for food pathogen detection. *Food Technol.* **2002**, *56* (3), 32–39.

(48) Personal communication and price enquiry with manufacturers.

(49) Sripawat, K.; Kaewpongso, S.; Suwanarusk, R.; Leimanis, M. L. Effective and cheap removal of leukocytes and platelets from *Plasmodium vivax* infected blood. *Malaria J.* **2009**, *8* (1), 115.